

## Effects of Differential Acylation and Polybasic Motif editing on Aberrant Growth Signaling by Overexpressed $\text{G}\alpha 13$

Nicholas White  
Biology Department  
The University of North Carolina Asheville  
One University Heights  
Asheville, North Carolina 28804 USA

Faculty Advisor: Dr. Ted Meigs

### Abstract

Overexpression of  $\text{G}\alpha 13$ , a member of the  $\text{G}12/13$  subfamily of heterotrimeric G proteins, has been implicated in cell transformation and the progression of several cancer types. The mechanism through which wildtype, overexpressed  $\text{G}\alpha 13$  drives aberrant growth signaling is not known. G protein  $\alpha$  subunits are modified post-translationally by acylation at the N-terminus, and this addition of a palmitoyl and/or myristoyl group occurs for all mammalian  $\text{G}\alpha$  proteins.  $\text{G}\alpha 13$  was previously engineered to mutate two cysteine residues necessary for dual palmitoylation. This modification abrogated signaling to serum response factor by  $\text{G}\alpha 13$  in both its wildtype and constitutively activated forms. To determine whether myristylation restores signaling to non-acetylated wildtype  $\text{G}\alpha 13$ , the protein was modified to harbor the 6 N-terminal amino acids from  $\text{G}\alpha T$ , which is myristoylated but not palmitoylated. Loss of growth signaling by non-palmitoylated, wildtype  $\text{G}\alpha 13$  was rescued by introduction of this myristoylated sequence. In addition, we used cellular fractionation to assess intracellular distribution of these  $\text{G}\alpha 13$  variants. Overexpressed, wildtype  $\text{G}\alpha 13$  showed a shift from a membrane associated fraction to a soluble pool, which correlated with a sharp increase in serum response factor signaling.  $\text{G}\alpha 13$  lacking any acylation sites localized entirely to the soluble fraction but exhibited no growth signaling. To query the nucleotide bound state of the soluble  $\text{G}\alpha 13$  pool, we combined cell fractionation with trypsin digestion assays. Surprisingly, overexpressed wildtype  $\text{G}\alpha 13$  in the soluble fraction was fully degraded, suggesting lack of GTP binding. These constructs have facilitated co-precipitation experiments to determine whether change in acylation state affects  $\text{G}\alpha 13$  binding to specific target proteins. E-cadherin and the RhoGEFs p115, PDZ and LARG were tested for their ability to bind  $\text{G}\alpha 13$  variants. Non-palmitoylated, constitutively active (QL)  $\text{G}\alpha 13$  was pulled down by all four proteins, evidence that its signal abrogation may be due to different cellular localization rather than reduced binding affinity. The wildtype version of this  $\text{G}\alpha 13$  construct appears to lose affinity to E-cadherin, though these results need to be explored further. Also examined was the role of an N-terminal polybasic motif in overexpressed wildtype  $\text{G}\alpha 13$  signaling, through amino acid substitutions in this region. Mutants were constructed using a non-palmitoylated variant of  $\text{G}\alpha 13$ , that inserted nine lysines upstream of the polybasic region. These constructs, called 9K, contained only an exaggerated positive region as a membrane signal and yet the QL type signaled almost as strongly as the positive control. Lastly, 3Q mutants were constructed to reduce the number of positively charged amino acids in the PBM region by converting them to glutamine. The wildtype version of this construct lost 80% of signal strength while QL was unaffected. These experiments demonstrate that rather than lipid membranes being a passive environment on which the dance of GPCR signaling occurs, lipid-protein interactions for  $\text{G}\alpha 13$  are crucial for its capacity to signal through SRE.

### 1. Introduction

In cellular signaling, heterotrimeric G proteins mediate the activation of G-protein coupled receptors (GPCRs) to various intracellular signaling pathways. G proteins consist of three subunits  $\alpha$ ,  $\beta$  and  $\gamma$ . The  $\beta$  and  $\gamma$  subunits form an irreversible dimer.  $\text{G}\alpha$  subunits have been organized into subfamilies based on sequence homology, including  $\text{G}\alpha_s$ ,  $\text{G}\alpha_i$ ,  $\text{G}\alpha_q$ , and  $\text{G}\alpha_{12/13}$ .<sup>1</sup> The  $\text{G}\alpha$  subunit acts as a molecular switch, binding to guanosine diphosphate (GDP) in its

inactive state, and guanosine triphosphate (GTP) in its active state. Activated  $\text{G}\alpha$  and free  $\text{G}\beta\gamma$  regulate effector proteins, RhGEFs and ion channels, as well as other downstream targets. Upon activation by an extracellular ligand, GPCRs undergo a conformational change which induces  $\text{G}\alpha$  to release GDP and bind GTP. Activated  $\text{G}\alpha$  has low binding affinity for both GPCRs and the  $\beta\gamma$  dimer and dissociates, diffusing across the membrane and activating signaling pathways.  $\text{G}\alpha$  subunits have intrinsic GTP hydrolysis activity, but this process is slow by nature. GTP hydrolysis and G protein inactivation is accelerated by GTPase activating proteins (GAPs). Hydrolysis of GTP to GDP inactivates  $\text{G}\alpha$  subunits, allowing reformation of the heterotrimer with the  $\beta\gamma$  dimer. G protein signaling is also modulated by another protein class: guanine nucleotide exchange factors (GEFs) which stimulate release of GDP allowing GTP to bind.

Membrane localization is a prerequisite for most currently known G protein functions. G proteins are modified after translation to incorporate various lipids, attached covalently, which serve to tether the protein to membranes via hydrophobicity. In addition, many G proteins contain a region of basic, positively charged amino acids known as a polybasic motif. These polybasic motifs allow for electrostatic adhesion to the negatively charged head groups of lipid membranes. While any one membrane binding signal may be weak, together these features can tether G proteins at cellular membranes, which is known as the two-signal hypothesis or kinetic trapping. Additionally, depending on the specific binding signals, different cellular membranes or membrane subdomain may be targeted. The regulation of these signals can modulate both membrane binding in general and which membrane is targeted for association.

The  $\text{G}\alpha_{12/13}$  subfamily has two members:  $\text{G}\alpha 12$  and  $\text{G}\alpha 13$ . Although in other G proteins, mutations are usually necessary for oncogenesis,  $\text{G}\alpha 13$  overexpression is sufficient to promote aggressive tumor growth and has been demonstrated in breast, oral, esophageal and colon cancer.<sup>2</sup> This makes the  $\text{G}_{12/13}$  family the most potent oncogenes of the  $\text{G}\alpha$  families.  $\text{G}\alpha 12$  and  $\text{G}\alpha 13$  activate cellular differentiation, migration and proliferation - all of which can drive metastasis and invasion if misregulated. Breast cancer progression and severity was linked to  $\text{G}\alpha 13$  signaling - promoting cytoskeletal rearrangements and activating downstream DNA transcription.<sup>3</sup>

This project seeks to answer two questions: What role does acylation play in  $\text{G}\alpha 13$  signaling and cancer progression? Why is overexpressed  $\text{G}\alpha 13$  oncogenic, whereas other G proteins require activating mutations? Nearly 20% of all human tumors have mutations in GPCRs and G proteins.<sup>4</sup> This research will give greater insight to how lipid modification regulates the function of  $\text{G}\alpha$  proteins and understanding these functions could illuminate critical targets for pharmaceutical compounds, changing the way the health industry treats cancer. Additionally, recent meta-analysis of the palmitoylome uncovered that 1,838 genes, or about 10% of the genome codes for palmitoylated proteins. These proteins were highly associated with several diseases including schizophrenia, Huntington's disease, and pancreatic ductal carcinoma. This suggests that palmitoylation and its misregulation plays an oversized role in regulating cell life and death and illuminating its role in  $\text{G}\alpha 13$  signal cascades could affect our understanding of neurological and oncological diseases.<sup>5</sup>

## 1.1 Myristylation

Myristylation is a co-translational modification of proteins by the irreversible addition of the 14-carbon saturated fatty acid myristic acid. After methionyl amino peptidase removes the methionine at position one, the consensus sequence  $\text{G}_2\text{-X}_3\text{-X}_4\text{-X}_5\text{-(S/T/C)}_6$  is recognized by N myristoyl transferase (NMT), which catalyzes the attachment of myristoyl-CoA through the free amide bond.<sup>6</sup> The amino acids at positions 3-7 can influence recognition by NMT. Although myristylation is irreversible, it is insufficient to promote stable membrane binding and requires combination with other targeting signals such as palmitoylation or polybasic motifs to keep proteins tethered - a phenomenon known as kinetic trapping, or the "two-signal" hypothesis. Myristylation in combination with polybasic motifs can allow for regulation of membrane binding via phosphorylation, which neutralizes the positive charge of the PBM and provides enough electrostatic repulsion to partition the proteins off the membrane in a process known as myristoyl electrostatic switching. Myristylation has demonstrably improved binding of  $\text{G}\alpha 1$  and  $\text{G}\alpha 0$  for By and is required for effective palmitoylation of  $\text{G}\alpha 1$ .<sup>7</sup>

## 1.2 Palmitoylation

Palmitoylation is the reversible, post-translational acylation of proteins by the saturated 16-carbon fatty acid palmitate, which attaches covalently to cysteines via a thioester bond. Although palmitate is only two carbons longer than myristate, palmitoylation provides an extremely stable tether to membranes. Hydrophobic binding energy of acylated polypeptides to artificial lipid micelles has been demonstrated to increase linearly with additional carbon chain length. Each  $\text{CH}_2$  added 0.825 kcal/mol of binding energy to phosphatidyl- choline (PC) vesicles. Notably the difference

between 16 and 14 carbon chains in terms of binding energy was 8 kcal/mol and 9.65 kcal/mol respectively, but this is sufficient to partition 99% of palmitoylated peptides into the membrane versus ~50% for myristoylated peptides as demonstrated by Peitzsch and McLaughlin.<sup>8</sup>

Palmitoylation does not have a consensus motif and is a modification for every G alpha subunit other than G $\alpha$ T and G $\alpha$ U. The DHHC proteins, named for a conserved motif at the enzymatic site, have demonstrated palmitoyl acyltransferase activity. DHHC3 and DHHC7 in particular are capable of catalyzing palmitoylation for G alpha subunits and siRNA mediated knockdown of these proteins led to loss of PM localization for G $\alpha$ q.<sup>3</sup> The half-life for palmitate attachment is short (~1 hour), variable and can be accelerated upon G protein activation. Palmitoylation-depalmitoylation cycles are an extremely important feature of G protein regulation as these cycles affect the cellular location of these proteins. Acyl protein thioesterase-1 (APT1) has been shown to depalmitoylate G $\alpha$ 13 and other G $\alpha$ . Research by Siegel et al 2009 showed that for dendritic spine morphogenesis, miRNA regulates the expression of APT1 leading to more palmitoylated, membrane bound G $\alpha$ 13.<sup>9</sup>

Table 1. Fatty acid modifications of G $\alpha$  and G $\gamma$  subunits

G $\alpha$ subunits	N-termini of subunits	Lipid modification	# lipids
$\alpha_{iL}$	<b>M</b> GCTLSAEDKAAVERS <span style="font-style: italic;">K</span> MID-	myristoylation, palmitoylation	m1p1
$\alpha_T$	<b>M</b> GAGASAEEKHSREL-	myristoylation	m1p0
$\alpha_{12}$	MSGVVRTLSR <b>C</b> LLPAEGAR-	palmitoylation	m0p1
$\alpha_{13}$	MADFLPSRSVLSV <b>C</b> FPGCVL-	palmitoylation	m0p2
G $\gamma$ subunits	C-termini of subunits	Lipid modification	# lipids
$\gamma_1$	-KGIPEDKNPF <b>K</b> ELKG <b>G</b> C_VIS	Farnesylation	f1
$\gamma_2$	-TPVPASENPFREKK <b>F</b> C_AIL	Geranylgeranylation	g1

Table 1: N terminal amino acid sequence of G proteins with respective lipid modifications, table modified from Wedegaertner.<sup>10</sup> Specific glycine side chains which are myristoylated are bold/underlined while palmitoylated residues are in bold italics. G $\gamma$  subunits are isoprenylated by either the 15-carbon farnesyl or the 20-carbon geranylgeranyl.

### 1.3 Polybasic Motifs

Polybasic motifs are stretches of basic, positive residues that act as an electrostatic anchor for membrane associated proteins. Although this makes them an irreversible membrane signal, it is possible to regulate their electrostatic potential (and thus membrane affinity) by phosphorylation of nearby residues. Some proteins take advantage of this fact by combining a polybasic motif with myristoylation. Neither signal provides enough binding energy to allow for permanent membrane residence, but together kinetic trapping is possible. When these proteins are phosphorylated, they partition rapidly off of the membrane - this is known as myristoyl electrostatic switching. G $\alpha$ Z is mono-lipidated by myristoyl and has a prominent polybasic motif. Additionally, G $\alpha$ Z can be phosphorylated at serines 17 and 27 which presumably affects its secondary structure and membrane affinity. Evidence to this effect is given by recent studies which show phosphorylated G $\alpha$ Z has reduced affinity for specific RGS proteins and with the G $\gamma$  subunits.<sup>11</sup>

The Meigs lab has developed a number of assays for interrogating G $\alpha$ 13. The serum response element (SRE) luciferase assay is a gene reporter assay which places the firefly protein luciferase gene downstream of a promoter element target called SRE. The G $\alpha$ 13 signaling cascade, which ends in serum response factor (SRF) driving gene expression, becomes converted into a fluorescent signal which can be measured by a luminometer. The basic experimental set-up in this project was to edit the coding DNA of G $\alpha$ 13 using PCR mutagenesis to abolish the native palmitoylation sites and to introduce the N-terminal amino acids from G $\alpha$ T which is only myristoylated. Previous work in the Meigs lab showed that G $\alpha$ 13 with the cysteine sites of palmitoylation replaced with alanine (a C14/18A mutant) failed to signal. Could this lipid swap from bi-palmitoylation to a single myristoyl group rescue signaling for non-acylated G $\alpha$ 13? Next, cell fractionation was used to roughly determine cellular localization. In this experiment,

HEK293 cells were transfected with  $\text{G}\alpha 13$  and snap-frozen with  $\text{N}_2$ . These cell lysates were then washed and ultracentrifuged. The soluble portion, which we predict contains mostly cytoplasmic proteins, is separated from the membranous, pelleted fraction, which presumably contain most of the cellular plasma membrane, Golgi, ER and other heavy organelles. The non-signaling C14/18A mutant was shown to delocalize from the membranous fraction to the soluble fraction, perhaps indicating that being membrane associated is a pre-requisite for  $\text{G}\alpha 13$  signaling. Strangely however, in cells with overexpressed  $\text{G}\alpha 13$ , a population of proteins spills over into the soluble fraction, which corresponds with a sharp increase in SRE signal.

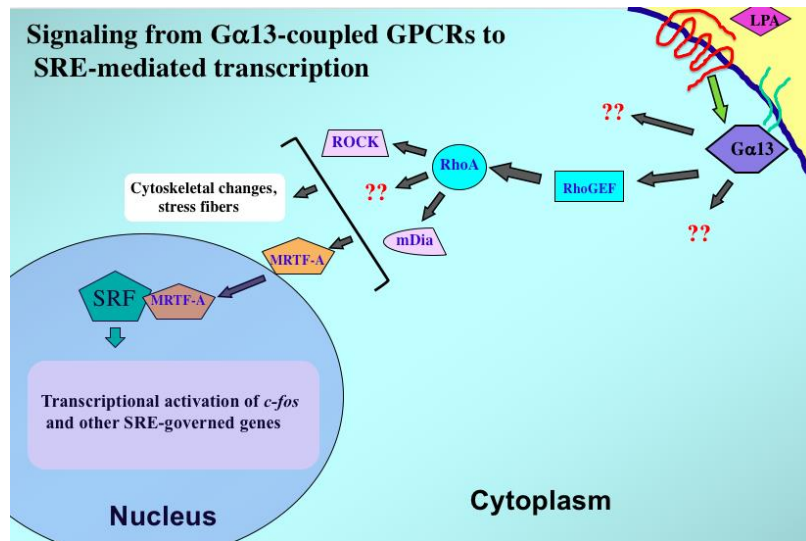


Figure 1: Serum Response Factor signaling cascade, repurposed with a plasmid harboring an SRE-governed luciferase coding sequence for signal strength measurements

Another hypothesis to explore was the possibility that the palmitoyl groups themselves were necessary to bind effector proteins. Co-protein immunoprecipitation experiments, informally known as protein pulldowns, were a useful diagnostic tool to this end. In this assay, effector proteins such as RhoGEFs are fused to a glutathione S-transferase tag (GST) and affixed to Sepharose beads. This Sepharose beads, which present the effector proteins on the surface like lollipop covered in sand, allow for  $\text{G}\alpha 13$  to bind tightly and then centrifuged out of solution, to be visualized by SDS-PAGE gels. As the project progressed other  $\text{G}\alpha 13$  mutants were created and tested using these assays, and a few other assays were attempted or planned such as trypsin digestion to query the GTP-bound status of G proteins and click chemistry to interrogate the palmitoylation status of  $\text{G}\alpha 13$  in the soluble fraction. In total, the combination of these experiments provide a compelling picture of the role palmitoylation and membrane-association more generally play for  $\text{G}\alpha 13$ .

## 2. Materials and Methods

### 2.1 Site directed PCR Mutagenesis.

$\text{G}\alpha 13$  QL-myc,  $\text{G}\alpha 13$  WT-myc,  $\text{G}\alpha 13$  C14/18A QL-myc,  $\text{G}\alpha 13$  C14/18A WT-myc were constructed in the Meigs lab previously, and used as templates for site directed mutagenesis.

### 2.2 Transformation.

JM109 *E.coli* cells were transformed in Falcon tubes while on ice with either 1  $\mu\text{L}$  of ligated plasmid or a no insert control and incubated for 30 min. After a 45 second heat shock at 42°C, the cells were returned to ice for 2 min, then outgrown in 0.9 mL of SOC medium in the 37°C incubator at 230 rpm for 1 hour. Liquid cultures were spun down at 9000xg for 3 min, the supernatant was decanted and the pellet resuspended in remaining (~100  $\mu\text{L}$ ) media. LB-

Ampicillin plates were covered with each transfection using glass beads after which the plates incubated for 12-16 hours and screened for colonies.

### 2.3 SRE-Luciferase Dual-Reporter Luminometric Assay.

In order to quantify how G13 constructs induce expression of genes controlled by SRE elements, HEK293 cells were grown to 80% confluence in 6-well plates and transfected with 200 ng SRE-luciferase plasmid, 200 ng Renilla plasmid pRL-TK, 100 ng Gα13 plasmid according to manufacturer's instructions included with the Lipofectamine 2000 transfection kit. For experiments involving  $\beta\gamma$ , cells were transfected with 200 ng of G protein construct +/- 200 ng  $\beta 1$  and 200 ng  $\gamma 2$ . Cells were grown for 36-48 hours. Cells were washed in Phosphate-buffered saline and suspended in passive lysis buffer (Promega) on a platform shaker for 25 minutes. Lysates were analyzed with a Dual-luciferase assay system and a GloMax 20/20 luminometer (Promega). Light output from SRE-Luciferase activity was divided by light from the renilla construct to control for constitutive expression. SDS-polyacrylamide gel electrophoresis and western blot analysis were used to control for relative protein expression in HEK293 cells which were subjected to the SRE luciferase assay.

### 2.4 Cell Fractionation:

HEK293 Cells were grown to 80% confluence in 10 cm dishes using Dulbecco's Modified Eagle's Media (Corning) and were transfected with Gα13 constructs using Lipofectamine 2000, incubated for 36-48 hours. Media was rinsed away with cold phosphate buffered saline and cells were scraped and suspended in 0.75 mL of PBS. Cells were pelleted by centrifugation at 500xg, 5 min, 2°C. Cell pellets were resuspended in 100 $\mu$ L Negishi Homogenization Buffer (20 mM Tris 7.4, 150 mM NaCl, 2 mM MgCl<sub>2</sub>, 1 mM DTT, 1x MP Biomedicals Protease Inhibitor Cocktail SKU#0215883701, 61  $\mu$ M TPCK, 58  $\mu$ M TLCK, 267  $\mu$ M phenylmethylsulfonyl fluoride) and 1:500 PI mix described elsewhere.<sup>13</sup> Cell homogenates were lysed by snap-freezing in liquid nitrogen and thawed in icy water. Samples were spun in a Sorvall vacuum ultracentrifuge at 100,000xg for ~20 minutes at 3°C. 50  $\mu$ L of supernatant was removed and set aside as the soluble fraction. Remaining supernatant was removed. Membrane pellet was resuspended in homogenization buffer, centrifuged at 100,000xg for ~20 minutes at 3°C. Supernatant was discarded, leaving a membrane fraction pellet. Cellular fractions were either analyzed by Western immunoblot or taken forward into the following trypsin protection assay.

### 2.5 Trypsin Protection

Membrane pellets from the previous fractionation procedure were sonicated for 3 minutes in 10 second on/off bursts keeping samples on ice. Trypsin digestion was carried out in 217 $\mu$ L HEDM Buffer (50mM HEPES, 1mM EDTA, 10mM MgSO<sub>4</sub>, 3mM DTT) 38 $\mu$ L of each fraction sample, and 24 $\mu$ L of 100ng/ $\mu$ L TPCK-Treated trypsin (New England Biolabs, Ipswich, MA) or ddH<sub>2</sub>O for negative control. Samples were heated for 20 minutes at 30°C, and proteolysis was terminated by addition of 10 $\mu$ L 100 mg/ml lima bean trypsin inhibitor (Worthington, Lakewood, NJ). Proteins were precipitated by 20% trichloroacetic acid and 0.8 mg/ml sodium deoxycholate. Samples were incubated on ice for 30 minutes and centrifuged at 100,000xg for ~20 minutes at 3°C. Supernatant was decanted until ~50 $\mu$ L remained and samples were centrifuged at 100,000xg for 3 minutes at 3°C. All supernatant was removed and pellets were washed with acetone, centrifuged for 15 min, 16,000xg, 3°C. Acetone was removed down to the last ~50 $\mu$ L and centrifuged for 5 min, 16,000xg, 3°C. Acetone was allowed to evaporate in a fume hood for ~2 hrs. Precipitated protein was suspended in 40 $\mu$ L 33% dilute SDS-PAGE 4x loading buffer with 100mM DTT, heated for 10 minutes at 72°C, and vortexed. Samples were analyzed by SDS-PAGE and immunoblotting using an Anti-Myc antibody (Millipore) and Anti-GNA13 antibody (Thermo-Fisher Scientific).

### 2.6 Co-immunoprecipitation

Extracts from transfected HEK293 cells were diluted in HEDM buffer (50 mM HEPES, pH 7.5, 1 mM EDTA, 3 mM dithiothreitol, and 1% polyoxyethylene-10-lauryl ether). Next, Sepharose-bound GST fusion proteins were added and continuously inverted for 2 hours at 4°C. A percentage of the diluted extract was set aside as starting material (i.e., load) before Sepharose addition. Samples were centrifuged at 1400g, and pellets were washed extensively and subjected to SDS-PAGE and immunoblot analysis using an Gα13 antibody (EMD Millipore) followed by alkaline phosphatase conjugated secondary antibodies (Promega, Madison, WI).

### 3. Results

#### 3.1 Non-Palmitoylated $\text{G}\alpha 13$ fails to signal through SRE and localizes to a soluble fraction

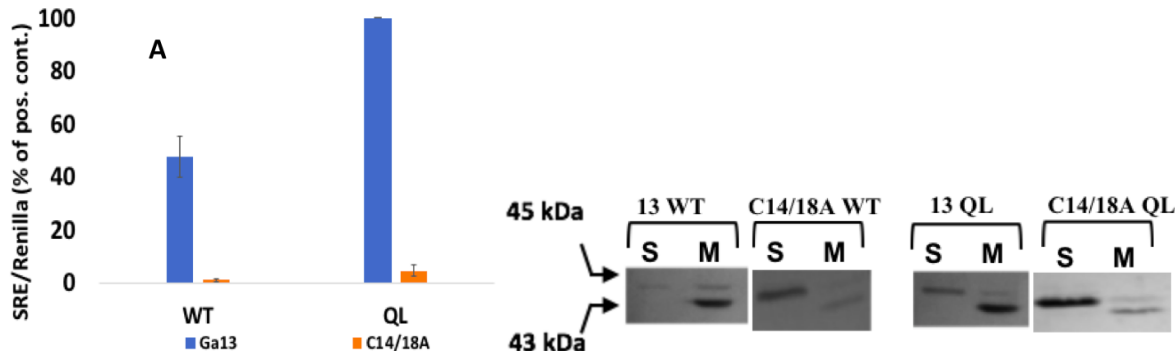


Figure 2: SRE signaling and cell fractionation for m0p2 and m0p0 WT and QL

Figure 2. A. Non-palmitoylated  $\text{G}\alpha 13$  localizes to a soluble fraction but fails to signal through SRF. We generated mutants of wildtype (WT) and constitutively activated (QL)  $\text{G}\alpha 13$  in which the native palmitoylation sites, Cys-14 and Cys-18, were mutated to alanine (C14/18A). Both variants were unable to signal to SRF, as measured in >3 luminometry experiments. Cell fractionations indicated this mutant form of  $\text{G}\alpha 13$  localized almost entirely to a soluble fraction. These data suggest the signaling capacity of the overexpressed wildtype  $\text{G}\alpha 13$  that “spills over” into a soluble fraction is not due solely to its presence in this fraction, and that its acylation state plays a key role in signaling to SRF. B. Engineering of  $\text{G}\alpha 13$  mutants with alternative acylation. To determine whether growth signaling by wildtype and activated (QL)  $\text{G}\alpha 13$  specifically requires palmitoylation, we introduced a myristylation site to our  $\text{G}\alpha 13$  mutants lacking palmitoylation sites. The six N-terminal amino acids of  $\text{G}\alpha 13$  were mutated to residues native to  $\text{G}\alpha T$  and  $\text{G}\alpha 1$ , and a third mutant was generated (termed Faith) in which a glycine at position 2 and serine at position 6 were introduced to create a consensus sequence for myristylation.<sup>12</sup>

#### 3.2 Additional Acylation Increases Signaling for $\text{G}\alpha 13$ Chimeras

PCR mutagenesis was used to introduce myristylation sites into  $\text{G}\alpha 13$  by mutating the first 6 N-terminal amino acids to those from  $\text{G}\alpha T$  and  $\text{G}\alpha 1$ . A third mutant was also made, “Faithful” which only changed the amino acids necessary to conform to the consensus sequence for myristylation. The coding sequence used contained a mutation previously engineered in the Meigs lab, a QL mutation at amino acid 226 which renders the subunit unable to hydrolyze GTP and therefore constitutively active. In order to control for transfection efficiency for samples within an experiment, SRE fluorescence is divided by renilla fluorescence. To compare results across experiments all fluorescence data is expressed as a percent % of the positive control QL. The negative control for signaling is a C14/18A mutant, wherein the cysteines required for palmitoylation are mutated to alanine. This non-acylated mutant fails to signal. In figure 1, graph A demonstrates through SRE luciferase assay that these introduced myristylation/palmitoylation sites increase SRE signaling, with the m1p3 (Gi/13) signaling more than either m1p2 mutant (faith, GT/13).

#### 3.3 Myristylation rescues signaling for non-palmitoylated $\text{G}\alpha 13$

Another set of mutants were engineered using the C14/18A, QL coding sequence of  $\text{G}\alpha 13$ , introducing one myristylation site (for GT/13 and Faithful) or one myristylation, one palmitoylation site (Gi/13). In figure 1, graph B, a single myristylation site (m1p0) is enough to rescue signaling for non-acylated  $\text{G}\alpha 13$  in the GT/13 mutant. The Faithful mutant did not recover signaling, possibly due lack of myristylation. In order to control for potential differences in transfection efficiency, the a portion of the cell lysates used for the SRE analysis was run on SDS-PAGE gels and analyzed by western blot. All  $\text{G}\alpha 13$  constructs all have an internal myc-tag, resulting in a heavier protein. It

is therefore easy to distinguish between genomic G $\alpha$ 13 which runs out at 43kDa and plasmid G $\alpha$ 13, at 45kDa (figure 1, **C&D**).

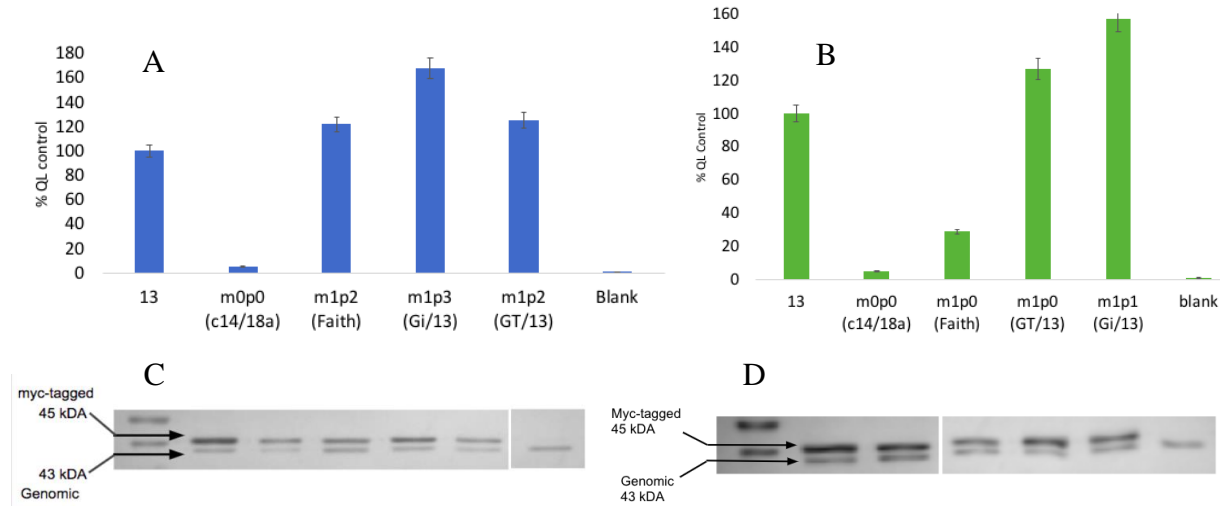
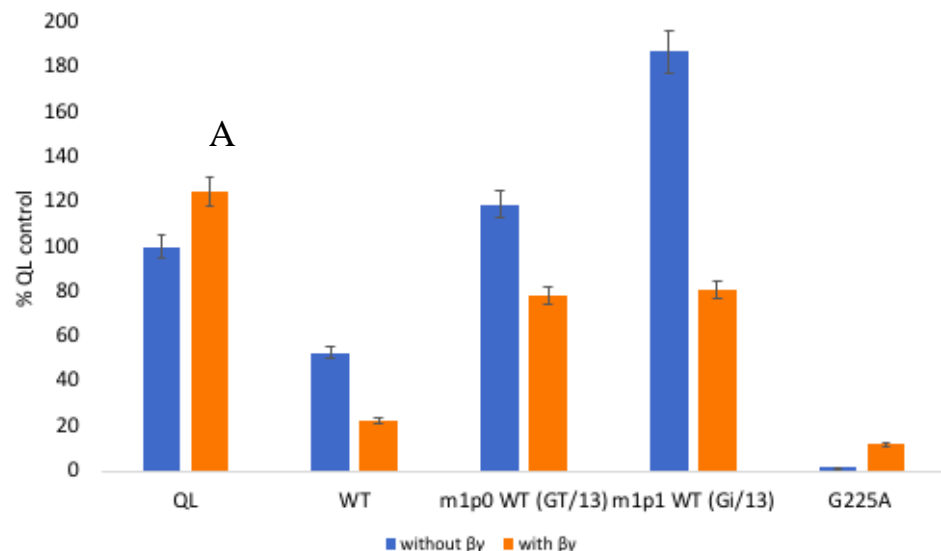


Figure 3: Dual glow SRE-Luciferase assay data for QL mutants.

Figure 3 **A**: “Doubled Up” constructs contain native G $\alpha$ 13 palmitoylation sites plus additional lipid attachments from N-terminal PCR engineering. **B**: Constructs have native G $\alpha$ 13 palmitoylation sites mutated to alanine and only contain novel lipidation site(s). **C,D**: Western blot showing expression of wildtype and chimeric G $\alpha$ 13, all proteins were detected at approximately equal levels.

### 3.4 Expressing $\beta$ Returns Soluble Fraction of Overexpressed G $\alpha$ 13 to plasma membrane and quenches signal for WT but not QL mutants

Previous work in the Meigs lab showed that transfecting HEK 293 cells with beta-gamma as well as G alpha could both return cytoplasmic fractions to the plasma membrane and quench signaling. Beta-gamma stabilizes the GDP bound state of G alpha proteins, inactivating them and also provides additional binding affinity for the plasma membrane. Additional PCR mutagenesis produced chimeras which were wildtype (WT) rather than QL. These were then tested in SRE assays, with and without beta-gamma. Most interestingly, myristoylated GT/13 and Gi/13 signaled much more strongly than G $\alpha$ 13 QL, indicating that localization may be a stronger factor than activating mutation for G protein signaling. Despite palmitoylation conferring more hydrophobic binding energy, the irreversibility of myristoylation seems to confer a greater advantage to signaling.



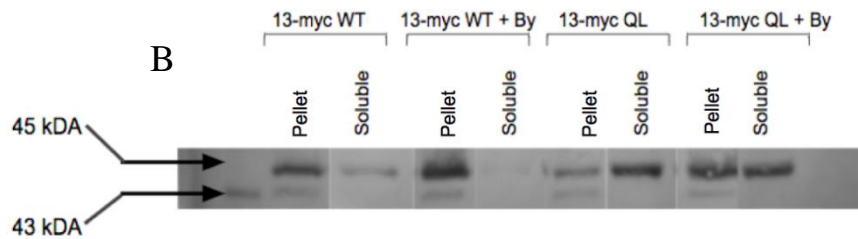


Figure 4: Dual-Glo SRE-Luciferase data for constructs +/-  $\beta\gamma$  and cellular fractionation

**Figure 4 A:** SRE signaling of Ga13 mutants, average of several experiments. Addition of  $\beta\gamma$  plasmids quenches signal for all mutants except 13QL, by binding to and stabilizing the GDP-bound, inactive form of the Ga13 mutants. Wildtype m1p0 and m1p1 signal more strongly than QL, indicating that the strength of lipid tether/cellular localization is more important for signaling. **B:** Cell fractionation was used to visualize cellular location of 13 WT and 13 QL with and without the presence of  $\beta\gamma$ . Overexpressed 13 spills into the soluble fraction and the addition of  $\beta\gamma$  returns much of the soluble fraction G13 back to the pellet fraction. The lower 43 kDa band is native Ga13, which is found entirely in the pellet fraction.

### 3.5 Protein Pulldowns

Previous work in the Meigs lab led to the creation of a library of known Ga13 effector proteins coupled with glutathione S-transferase (GST) tags. These GST tags allow the proteins to bind to Sepharose beads. These beads expose the effector proteins on their surface allow for the binding of Ga13 in cellular lysate preparations. Then the beads are pulled down and separated by centrifugation, to be tested later via SDS-PAGE and western blot. In this way, many G protein variants can be screened for their binding capacity to known G protein effectors simultaneously. Such effectors include leukemia associated RhoGEF (LARG), p115 RhoGEF, PDZ RhoGEF, n-radixin and E-cadherin. To control that the beads themselves are not binding the proteins, blank GST beads are tested for each G protein variant, and each G protein has a separate load sample to control for relative abundance from transfection. Coomassie blue staining was also used to control for amount of protein in each interaction tube.

#### 3.5.1 Palmitoylation status does not affect binding for 13 QL to RhoGEFs

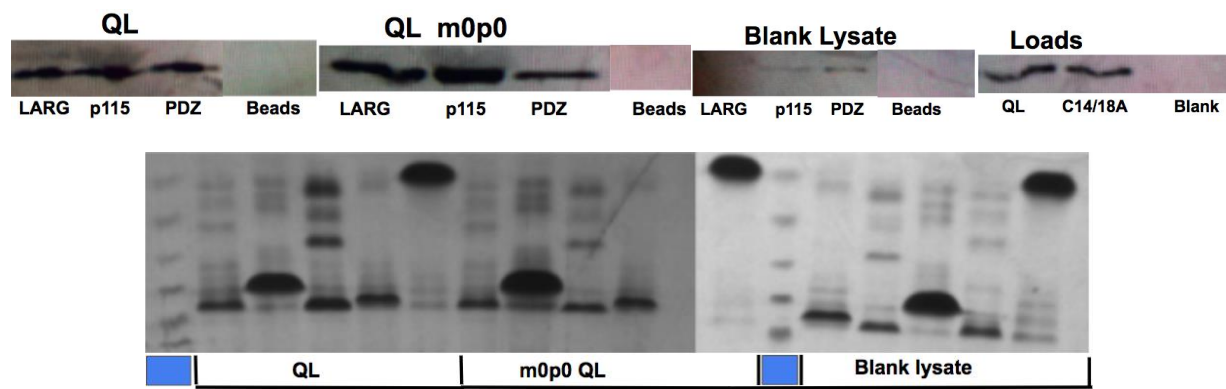


Figure 5: Protein pulldown for 13 QL, 13 c14/18a and blank lysates. Lanes with blue squares contain protein ladder

Figure 5: 13 QL (m0p2) and c14/18a QL (m0p0) were tested for their ability to bind LARG, p115 RhoGEF, PDZ RhoGEF and N-radixin. N-radixin failed to bind either the positive control 13 QL or m0p0 QL and was left out of later experiments. Both palmitoylated and non-palmitoylated active Ga13 bound to LARG, p115 and PDZ effectively.

This data seems to indicate that palmitoylation status does not affect binding affinity, at least for these effectors, and that non-lipidated 13 fails to drive SRE signaling due to proximity, i.e. not being membrane bound.

### 3.5.2 Myristoylated 13 QL binds to p115 and PDZ RhoGEFs

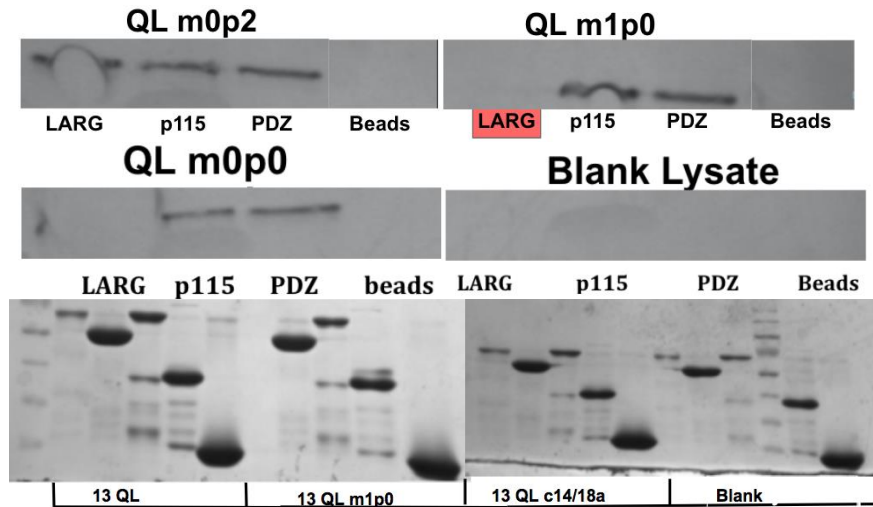


Figure 6: Protein Pulldown(s) and Coomassie blue stain for 13 QL, m1p0 QL, and m0p0 QL against LARG, p115, PDZ and E-cadherin. The LARG-QLm1p0 interaction tube did not contain protein as seen in the Coomassie blue stain, lane 6, after the ladder and therefore the sample is a false negative.

### 3.5.3 13 WT C14/18A fails to bind to LARG and E-Cadherin

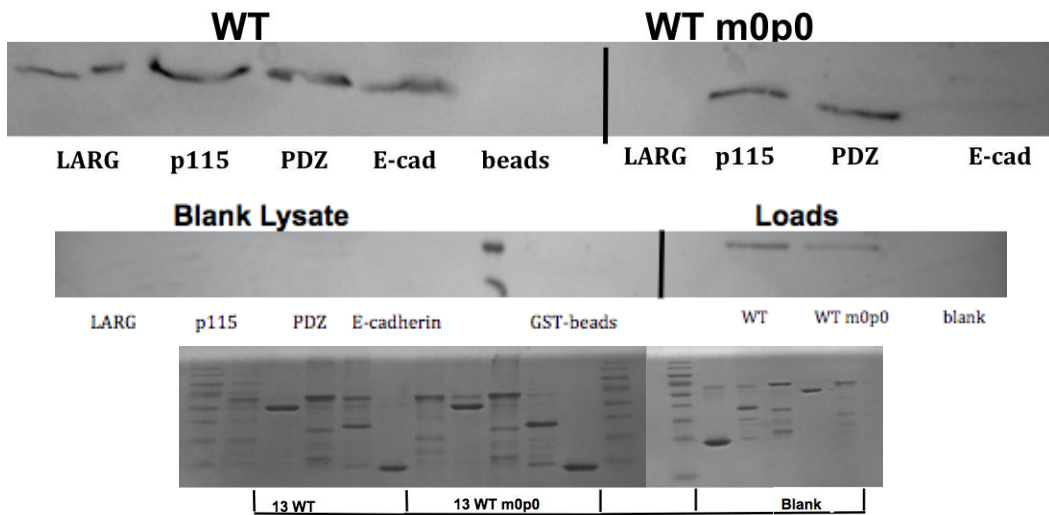


Figure 7: WT 13 pulldowns with RhoGEFs and E-cadherin.

Figure 7: 13 WT is pulled down by leukemia associated RhoGEF (LARG), PDZ RhoGEF, PDZ RhoGEF and E-cadherin. Non-acylated WT failed to be pulled down by LARG and E-cadherin. Other pulldowns have shown that LARG may be capable of binding to WT m0p0 but E-cadherin has not been shown to bind this mutant at this time.

### 3.7 Identification of the polybasic motif in G $\alpha$ 13

Previously it had been hypothesized that G proteins require either a myristoyl group or a polybasic motif in order to be kinetically trapped at the membrane. Myristylation, which occurs co-translationally, and PBMs serve to provide a transient membrane association to the Golgi. Next, alpha subunits are palmitoylated, bind to  $\beta\gamma$  and the heterotrimer is sent to the plasma membrane via endosomes. Polybasic motifs have also been described as membrane orientation patches and their ability to bind effectively to different lipid species is still being researched. Notably, these regions can also contain negatively charged amino acids though whether these are necessary for stabilization of the alpha helix or provide a means of discrimination for zwitterionic headgroups remains to be seen. Research by Kosloff et al. in 2002 showed evidence that a polybasic motif may exist for G $\alpha$ 13 and other palmitoylated alpha subunits by overlaying electrostatic data from amino acid sequences onto an averaged G protein structure (since some have not been fully crystallized).<sup>13</sup> If a polybasic motif did exist for G $\alpha$ 13 it would be necessary to (re)-identify it in order to make mutant G $\alpha$ 13 which could probe this region. The N-terminus of G $\alpha$ 13 has never been crystallized, making inference about any polybasic motif difficult. However, with the use of some bioinformatics tools and some inference, a possible polybasic motif was indeed discovered for G $\alpha$ 13.

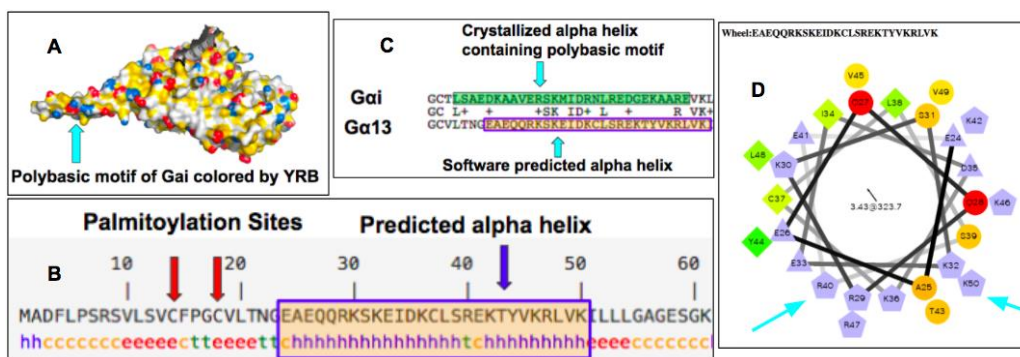


Figure 8: The polybasic motif (PBM) in G $\alpha$ 13 (re)-discovered

Figure 8: A: The side chains in G $\alpha$ i were colored by the Pymol program YRB: showing atoms which are hydrophobic (yellow), positive (blue) and negative (red). B: The amino acid sequence for G $\alpha$ 13 was run through the structure prediction software SOPMA, and an alpha helix near the two palmitoylation sites was discovered to have 9 positive side chains. C: Protein sequence for G $\alpha$ i and G $\alpha$ 13 were aligned by BLASTp. The polybasic crystallized alpha helix for G $\alpha$ i overlapped almost perfectly with the predicted PBM alpha helix for G $\alpha$ 13. D: The predicted PBM alpha helix was run through helical wheel projection software, demonstrating the positively charged side chains (shown in violet pentagons) aligned on one side.

### 3.9 An exaggerated polybasic motif rescues non-lipidated QL but not WT signaling. Muted polybasic motif suppresses WT but not QL m0p2 signaling.

The existence of the polybasic patch in G $\alpha$ 13 begged several questions. How strong was the electrostatic attraction of this alpha helix to the Golgi? How would signaling be affected if this feature was weakened or strengthened? Could signaling for G $\alpha$ 13 be restored with just electrostatics rather than palmitoylation or myristylation? Two pairs of mutants were engineered, the first with megaprimer PCR mutagenesis and the second with overlap extension (sewing) PCR. QL and WT mutants lacking palmitoylation sites were engineered with a span of nine Lys residues near the N-terminus, inserted just upstream of its putative polybasic motif. The next set of QL/WT pair mutants took an RKS $\mathbf{K}$  motif at the beginning of the alpha helix and mutated it to QQLQ. Respectively, these features which exaggerated and suppressed positive charge were termed 9K and 3Q.

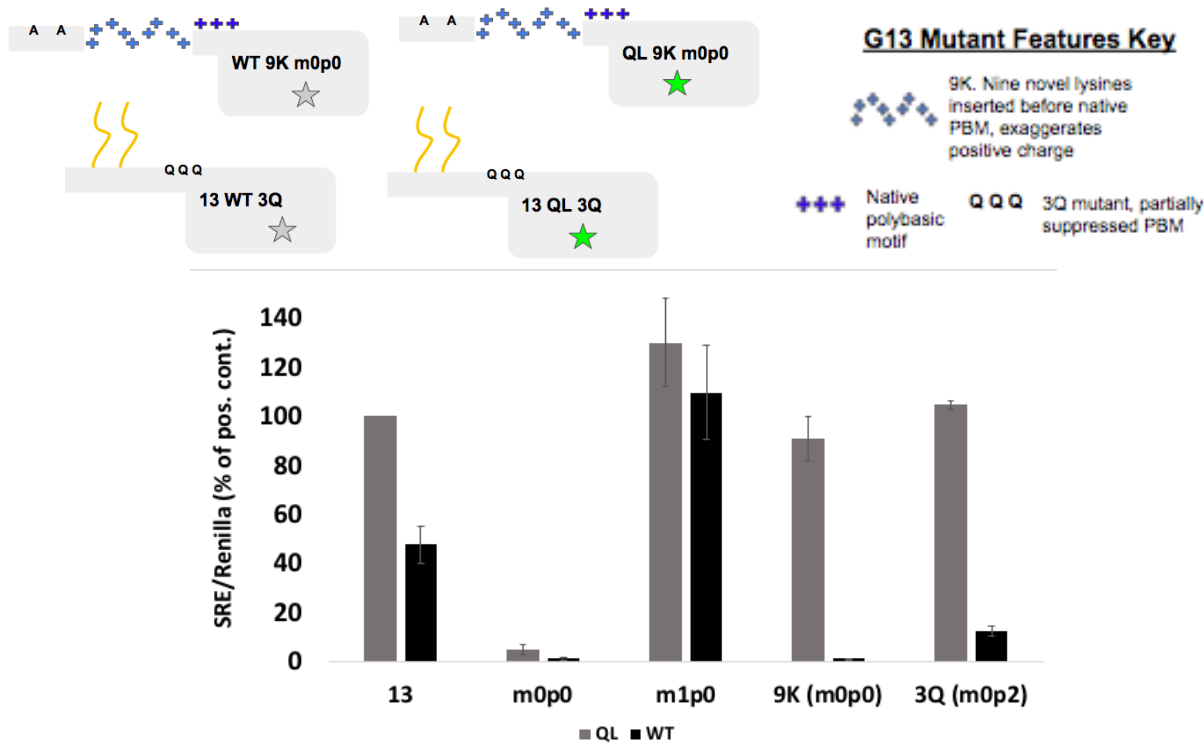


Figure 9: Dual Glo SRE for QL and WT variants of 13 mutants including m1p0, 9K (m0p0) and 3Q (m0p2).

Figure 9. **(Top)** Visualization of the 9K and 3Q mutant pairs. **(Bottom)** An exaggerated polybasic motif rescues SRF signaling for non-acylated  $\text{G}\alpha 13$ . A mutant with a span of nine Lys residues near the N-terminus of  $\text{G}\alpha 13$  was engineered, just upstream of its putative polybasic motif. This insertion (termed 9K) fully rescued signaling for activated (QL)  $\text{G}\alpha 13$  lacking the palmitoylated Cys residues; however the wildtype form of this  $\text{G}\alpha 13$  construct showed no SRF signaling. Furthermore, charge-loss of existing components of the native polybasic region in  $\text{G}\alpha 13$  (residues RKS to QSQ) was disruptive to SRF signaling by wildtype  $\text{G}\alpha 13$  but not activated (QL)  $\text{G}\alpha 13$ . These mutants (termed 3Q) retained their native palmitoylation sites, Cys-14 and Cys-18. Results are from two or more independent experiments per construct, and error bars indicate s.e.m.

## 4. Future Work

### 4.1 Querying Palmitoylation of overexpressed, soluble $\text{G}\alpha 13$ via click chemistry/cell fractionation

Overexpressed  $\text{G}\alpha 13$  spills over into the soluble fraction in cell fractionation experiments, corresponding with a sharp increase in SRE signaling. However, non-acylated  $\text{G}\alpha 13$  which localizes entirely to the soluble fraction fails to signal. In order to query whether overexpressed soluble fraction  $\text{G}\alpha 13$  is palmitoylated, a click chemistry assay was designed. Click-chemistry is a reaction designed by chemical biologists to study acylation with little disruption to normal cellular processes. First, an alkyne analog is incubated with transfected HEK293 cells, starved of fatty acids. Proteins which are palmitoylated uptake this analog. Next, the cells are washed and incubated with azide-biotin, sodium ascorbate,  $\text{CuSO}_4$  and THPTA. Sodium ascorbate oxidizes the  $\text{Cu(I)}$  to  $\text{Cu(II)}$  which acts as a catalyst to cyclize a 5 membered ring between the alkyne group and the azide. The cells are snap frozen in liquid  $\text{N}_2$ , separated into soluble and membrane fractions by ultracentrifugation and the  $\text{G}\alpha 13$  molecules separated by their myc tags using anti-myc Sepharose beads. Then after running SDS-PAGE, the blots can be visualized by washing with streptavidin-AP, which will bind to the biotin group of palmitoylated proteins.

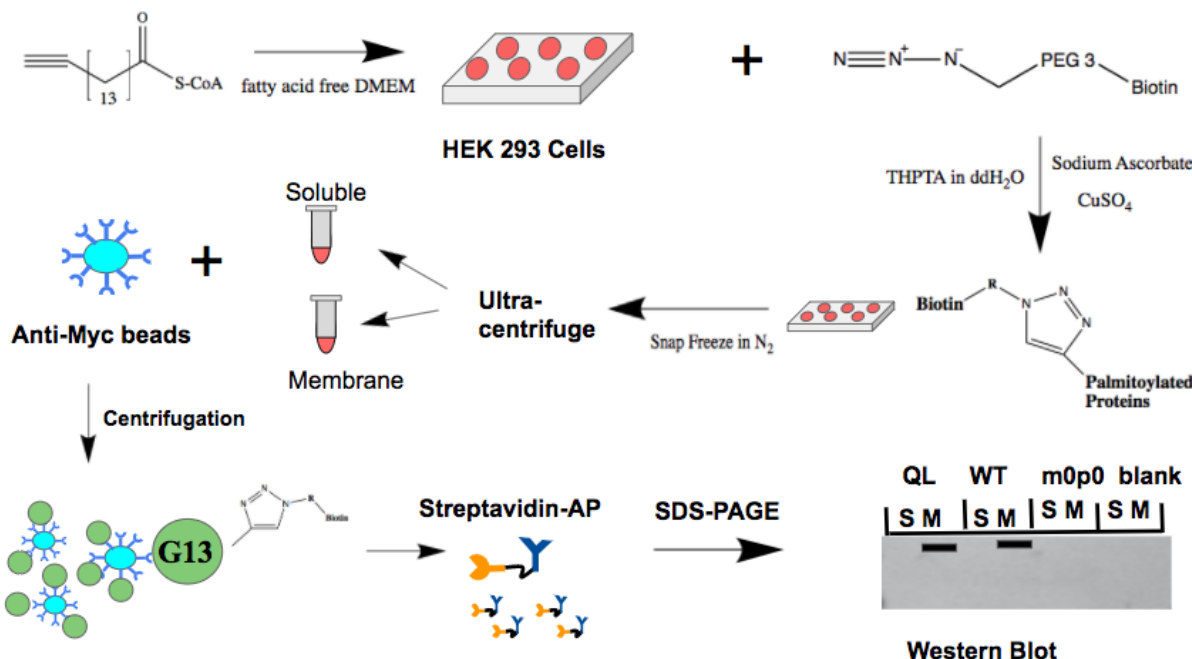


Figure 10. Experimental Design to query G $\alpha$ 13 palmitoylation status in membrane and soluble fractions via click chemistry. HEK293 cells transfected with myc-G $\alpha$ 13 mutants will be incubated with alkyne-palmitoyl after a period of fatty acid starvation. Azide-Biotin will be reacted with alkyne-palmitoyl using CuSO<sub>4</sub>, sodium ascorbate and THPTA. Cells will be separated into membranous and soluble fractions as shown in Fig. 5. Anti-myc beads will be used to isolate myc-tagged G $\alpha$ 13 from other palmitoylated proteins in solution. Samples will be separated by SDS-PAGE/electroblotting and probed using AP-streptavidin to detect G $\alpha$ 13 palmitoylation.

## 5. Conclusion

The primary role of palmitoylation is to tether G $\alpha$ 13 to the membrane where it can bind to  $\beta\gamma$ , GPCRs, RhoGEFs and other downstream targets efficiently. The labile thioester bond allows regulation of these palmitoyl groups by Acyl Protein Thioesterases such as APT1 and added by palmitoyltransferase DHHC family. Removing these sites by PCR mutagenesis results in G $\alpha$ 13 localizing to the soluble fraction and corresponds with a near total lack of SRE signaling. Several additional mutants, both wildtype and the constitutively active QL variant, were engineered to contain either a single myristoyl site (m1p0) or a myristoyl and palmitoyl site, in the case of Gi/13 (m1p1). The addition of this myristoylation site recovered SRE signaling, especially the GT/13 mutant (m1p0). This mutant, though it only contained the binding capacity afforded from a single myristoyl group and a polybasic patch signaled about the same as the ‘hyper-acylated’ mutants which were either m1p2 or m1p3, mostly like due to diminishing returns from tether strength (kinetically trapping a protein 99% of the time versus 99.999% of the time would make little difference).

In order to control for the possibility of stoichiometric imbalance between G $\alpha$ 13 and  $\beta\gamma$ , and thus atypical rates of heterotrimer formation, SRE signaling was tested both with and without co-transfection of  $\beta\gamma$ . These experiments were combined with cell fractionation and demonstrated that  $\beta\gamma$  both quenched WT signaling and dragged a portion of soluble overexpressed G $\alpha$ 13 back to the membrane.  $\beta\gamma$  was also shown to increase the population of 13 QL in the membranous fraction, but this also led to an *increase* in signaling, a result duplicated many times now in the Meigs lab. One possible explanation is that overexpressed G $\alpha$ 13 may become ‘stuck’ at the Golgi waiting for a  $\beta\gamma$  pair in order to form a heterotrimer and reach the membrane. The addition of overexpressed  $\beta\gamma$  relieves this pressure and the flux of the heterotrimer to the plasma membrane increases. There the QL mutant, still GDP bound at this point, becomes activated by a GPCR and assume its stable GTP bound form.

To test whether these acyl groups were involved in protein-protein interactions, co-immunoprecipitation experiments were conducted with LARG, p115, PDZ and E-cadherin. QL m0p0 appears to bind RhoGEFs effectively, and further experimentation will determine its capacity to bind to E-cadherin. This indicates that SRE signal is

abrogated for non or de-palmitoylated  $\text{G}\alpha 13$  due to a localization problem, rather than a decrease in binding affinity. However,  $\text{G}\alpha 13$  WT m0p0 appears unable to bind to LARG and E-cadherin. Though subsequent experimentation has shown some affinity for LARG, this mutant has been unable to bind effectively to E-cadherin (data not shown). It is possible that E-cadherin, a transmembrane protein, binds not only to  $\text{G}\alpha 13$  below the inner leaflet of the plasma membrane, but also one or more of the palmitoyl groups within the membrane and that removing these acyl chains disturbs effective binding. Lastly, a possible polybasic motif for  $\text{G}\alpha 13$  was discovered and interrogated. Exaggerated positive charge was able to rescue 13QL m0p0 but this is most likely due to the fact that the QL membrane allows for short-cutting of the usual signal transduction of active GPCR  $\rightarrow \text{G}\alpha\beta\gamma \rightarrow$  active  $\text{G}\alpha$  and that even a transient membrane association could allow for successful binding and SRE signaling. Indeed, the WT version fails entirely to signal, like due from a disrupted binding to either activated GPCRs or  $\beta\gamma$ .

A putative polybasic motif for  $\text{G}\alpha 13$  was shown using a bioinformatical approach using comparison to a  $\text{G}\alpha i$  crystal structure, predicting the N-terminal structure of  $\text{G}\alpha 13$  using SOPMA, pairwise analysis of amino acid sequence between  $\text{G}\alpha 13$  and  $\text{G}\alpha i$ , and finally a helical wheel diagram demonstrating alignment of the charged residues on one face of the alpha helix. In order to test the exaggeration and muting of this electrostatic tether, 9K and 3Q mutants were created. Surprisingly, the exaggerated PBM was able to rescue SRE signaling for QL but not for WT. The muted 3Q had no effect on QL signaling but knocked down the WT signal to about half of its control.

Immediate future work includes a detailed click chemistry reaction for querying the palmitoylation of the soluble fraction of overexpressed  $\text{G}\alpha 13$ . Additional co-immunoprecipitation and cell fractionation experiments will also be performed in the near future. Next, the research could take a few different experimental paths including testing the effect disrupting lipid rafts has on  $\text{G}\alpha 13$ . Methyl- $\beta$ -cyclodextrin is a well-known cholesterol synthesis inhibitor which disrupts lipid raft formation. The Meigs lab has also recently acquired a flow cytometer and is in the process of developing assays for this equipment. Two possibilities include quantification of SRE signal using a destabilized GFP protein with a short (~2hr) half-life and developing  $\text{G}\alpha 13$ /binding partner fluorescent protein pairs for FRET analysis. There are many remaining questions for  $\text{G}\alpha 13$  and the roles its membrane targeting signals play. Recently, the effects of membrane microdomains such as the  $\text{H}_{\text{II}}$  phase have been suggested to play a role in G protein signaling – an intriguing possibility the Meigs lab may be able to study.

## 6. Acknowledgements

The author wishes to express their appreciation to Dr. Ted Meigs, without whom none of this could have been accomplished. Any success is due to his tireless guidance and teaching. Also, many thanks goes out to the other researchers in Dr. Meigs lab including Beka Stecky, Courtney Quick, Katie Brown, Sam Nance, Mackenzie Mull, Corin O’Shea, and Nicole Dover.

## 7. References

- 1 Wedegaertner, “G Protein Trafficking.”
- 2 Wedegaertner.
- 3 Kelly et al., “The G12 Family of Heterotrimeric G Proteins Promotes Breast Cancer Invasion and Metastasis.”
- 4 O’Hayre et al., “The Emerging Mutational Landscape of G Proteins and G-Protein-Coupled Receptors in Cancer.”
- 5 Sanders et al., “Curation of the Mammalian Palmitoylome Indicates a Pivotal Role for Palmitoylation in Diseases and Disorders of the Nervous System and Cancers.”
- 6 Wedegaertner, “G Protein Trafficking.”
- 7 Chen and Manning, “Regulation of G Proteins by Covalent Modification.”
- 8 Peitzsch and McLaughlin, “Binding of Acylated Peptides and Fatty Acids to Phospholipid Vesicles.”
- 9 Siegel et al., “A Functional Screen Implicates MicroRNA-138-Dependent Regulation of the Depalmitoylation Enzyme APT1 in Dendritic Spine Morphogenesis.”
- 10 Wedegaertner, “G Protein Trafficking.”
- 11 Chen and Manning, “Regulation of G Proteins by Covalent Modification.”
- 12 Bhattacharyya and Wedegaertner, “ $\text{G}\alpha 13$  Requires Palmitoylation for Plasma Membrane Localization, Rho-Dependent Signaling, and Promotion of P115-RhoGEF Membrane Binding.”

---

13 Kosloff, Elia, and Selinger, "Structural Homology Discloses a Bifunctional Structural Motif at the N-Termini of G  $\alpha$  Proteins †."